

## Research Article

# Numerical Modelling of Squeeze Film Performance between Rotating Transversely Rough Curved Circular Plates under the Presence of a Magnetic Fluid Lubricant

**Nikhilkumar D. Abhangi<sup>1</sup> and G. M. Deheri<sup>2</sup>**

<sup>1</sup> *Department of Mathematics, Faculty of Engineering, Marwadi Foundation Group of Institutions, Rajkot 360 003, Gujarat State, India*

<sup>2</sup> *Department of Mathematics, Sardar Patel University, V. V. Nagar-388120, Gujarat State, India*

Correspondence should be addressed to Nikhilkumar D. Abhangi, [nikhil.abhangi@gmail.com](mailto:nikhil.abhangi@gmail.com)

Received 13 May 2012; Accepted 8 August 2012

Academic Editors: S. Cartmell, J. Hu, and R. Nagaosa

Copyright © 2012 N. D. Abhangi and G. M. Deheri. This is an open access article distributed under the Creative Commons Attribution License, which permits unrestricted use, distribution, and reproduction in any medium, provided the original work is properly cited.

An endeavour has been made to study and analyze the behaviour of a magnetic fluid-based squeeze film between curved transversely rough rotating circular plates when the curved upper plate lying along a surface determined by an exponential function approaches the curved lower plate along the surface governed by a secant function. A magnetic fluid is used as the lubricant in the presence of an external magnetic field oblique to the radial axis. The random roughness of the bearing surfaces is characterised by a stochastic random variable with nonzero mean, variance, and skewness. The associated nondimensional averaged Reynolds equation is solved with suitable boundary conditions in dimensionless form to obtain the pressure distribution, leading to the expression for the load carrying capacity. The results establish that the bearing system registers an enhanced performance as compared to that of the bearing system dealing with a conventional lubricant. This investigation proves that albeit the bearing suffers due to transverse surface roughness, there exist sufficient scopes for obtaining a relatively better performance in the case of negatively skewed roughness by properly choosing curvature parameters and the rotation ratio. It is appealing to note that the negative variance further enhances this positive effect.

## 1. Introduction

Archibald [1] presented a study on the squeeze film behaviour between various geometrical configurations of flat surfaces. Hays [2] modified the analysis of Archibald [1] to discuss the squeeze film phenomena between curved plates considering the curvature of sine form and keeping minimum film thickness as constant. Murti [3] investigated the squeeze film performance in curved circular plates describing the film thickness by an exponential expression. Indeed, his analysis was based on the assumption that the central film thickness instead of minimum film thickness considered by Hays [2] was constant. It was established that the load carrying capacity rose sharply with the curvature in the case of concave pads. In the above investigation the lower plate was assumed to be flat. Ajwaliya [4] extended

the analysis of Murti [3] by choosing the lower plate along a surface determined by an exponential function. Patel and Deheri [5] developed this approach to analyze the squeeze film behaviour between curved circular plates lying along the surfaces determined by hyperbolic function. The analysis of Murti [3] was simplified to a larger extent by Prakash and Vij [6] by incorporating the well-known Morgan-Cameron approximation when the porous facing thickness was considered small.

Wu [7] investigated the effect of rotation between squeeze film behaviour in porous annular disks and showed that rotation caused reduced load carrying capacity as well as response time. Bhat and Patel [8] modified the approach of Wu [7] to study the effect of axial current-induced pinch on the lubrication of rotating porous annular and circular disk. Subsequently, Vora and Bhat [9] analyzed the load carrying

capacity of a squeeze film between curved porous rotating circular plates by extending the analysis of Prakash and Vij [6].

Conventional lubricants were used in all the above investigations. The application of magnetic fluid as a lubricant was investigated by Verma [10] and Agrawal [11]. The magnetic fluid consisted of magnetic grains suspended in a magnetically passive solvent coated with a surfactant. Bhat and Deheri [12] presented the study of squeeze film behaviour between porous annular disks using a magnetic fluid lubricant with the external magnetic field oblique to the lower disk. Here in this investigation it was found that the application of magnetic fluid as a lubricant enhanced the performance of the squeeze film significantly. However, the plates were considered to be flat. But in actual practice the flatness of the plate does not endure due to elastic, thermal and uneven wear effects. Taking this point into account Bhat and Deheri [13] studied the effect of a magnetic fluid lubricant on the configuration of Ajwaliya [4] by considering the two plates along the surfaces described by exponential functions. Here also, it was established that the load carrying capacity rose sharply due to the magnetic fluid lubricant. Patel and Deheri [14] modified the approach of Bhat and Deheri [13] to analyze the behaviour of a magnetic fluid-based squeeze film between curved annular plates by taking the curvature governed by hyperbolic form. Patel and Deheri [15] observed the magnetic fluid-based squeeze film behaviour between curved circular plates lying along a surface determined by secant functions. All these investigations underlined the importance of the curvature parameter for improving the performance of bearing system. Squeeze film performances are used in skeletal joints, bio-lubrication, extending the frequency of sensor and ear.

It is a well-known fact that particularly after having some run-in and wear the bearing surfaces develop roughness. Even the contamination of the lubricant and chemical degradation of the surfaces result in roughness. It is also a well-established fact that the randomness of the roughness and the multiple roughness scales both contribute to the complexity of the geometrical structure of the surface. Invariably, it is this complexity which contributes to most of the problem in studying and analyzing friction and wear. The random character of the surface roughness was recognized by several investigators who resorted to a stochastic approach for modelling the roughness (Tzeng and Saibel [16], Christensen and Tonder [17–19], Tonder [20]). Tzeng and Saibel [16] made use of a beta probability density function for the random variable characterizing the roughness. This distribution appears to be symmetrical in nature with nonzero mean. Christensen and Tonder [17–19] further developed and extended this approach of Tzeng and Saibel [16] to present a comprehensive general analysis both for transverse as well as longitudinal surface roughness. A good number of investigations (Tonder [20], Ting [21], Prakash and tiwari [22], Prajapati [23], Guha [24]) adopted this approach of Christensen and Tonder [17–19] to develop the frame work for analyzing the effect of surface roughness on the performance of squeeze film behaviour. Andharia, Gupta, and Deheri [25] discussed the

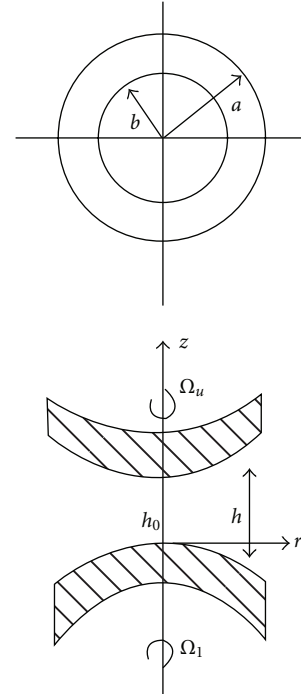


FIGURE 1: Configuration of the bearing system.

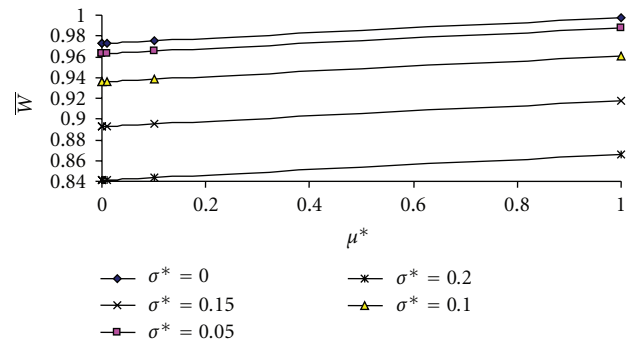


FIGURE 2: Load carrying capacity with respect to  $\mu^*$  and  $\sigma^*$ .

effect of transverse surface roughness on the performance of a hydrodynamic squeeze film in a spherical bearing using the general stochastic analysis. It was observed that the effect of transverse surface roughness on the performance of the bearing system was relatively adverse.

Andharia [26] dealt with the squeeze film behaviour between rotating porous circular plates with a concentric circular pocket and studied the combined effect of elastic deformation and surface roughness. Prajapati [27] discussed the effect of surface roughness and rotational inertia on the optimal stiffness of hydrostatic thrust bearing. Lin, and Chinang [28] considered the effect of rotation on the performance of a magnetic fluid-based circular step bearing considering the bearing surfaces to be transversely rough.

Here it has been proposed to investigate the behaviour of a magnetic fluid-based squeeze film in rotating curved rough circular plates where in the upper surface is determined by an

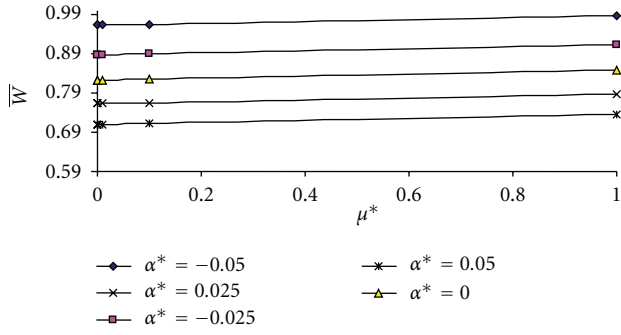


FIGURE 3: Load carrying capacity with respect to  $\mu^*$  and  $\alpha^*$ .

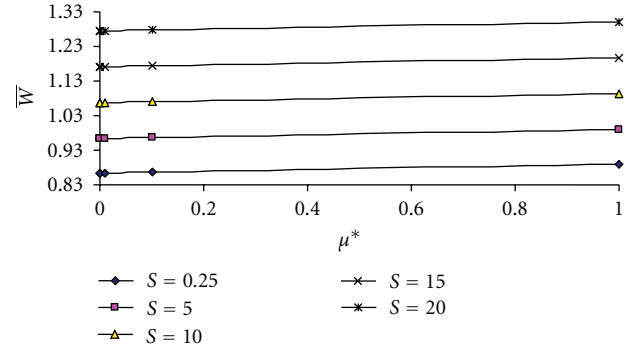


FIGURE 7: Load carrying capacity with respect to  $\mu^*$  and  $S$ .

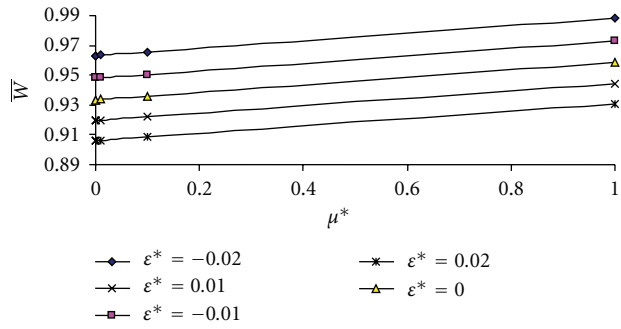


FIGURE 4: Load carrying capacity with respect to  $\mu^*$  and  $\epsilon^*$ .

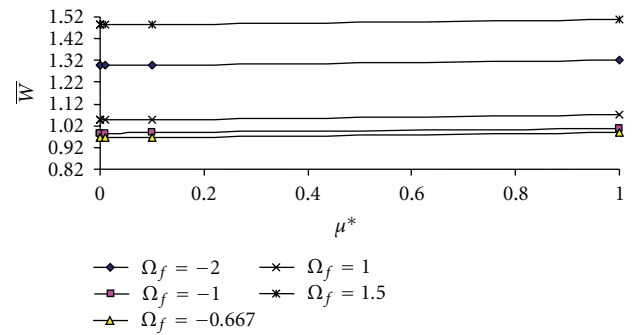


FIGURE 8: Load carrying capacity with respect to  $\mu^*$  and  $\Omega_f$ .

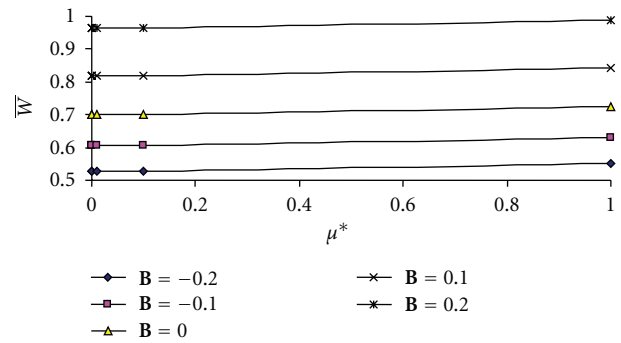


FIGURE 5: Load carrying capacity with respect to  $\mu^*$  and  $B$ .

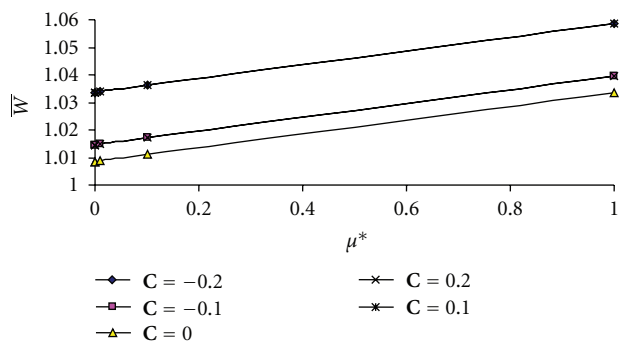


FIGURE 6: Load carrying capacity with respect to  $\mu^*$  and  $C$ .

exponential expression while the surface of the curved lower plate is governed by a secant function.

## 2. Analysis

The geometrical configuration of the rotating bearing system is displayed in Figure 1.

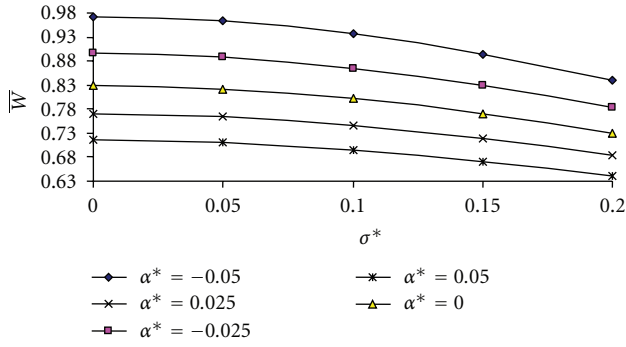
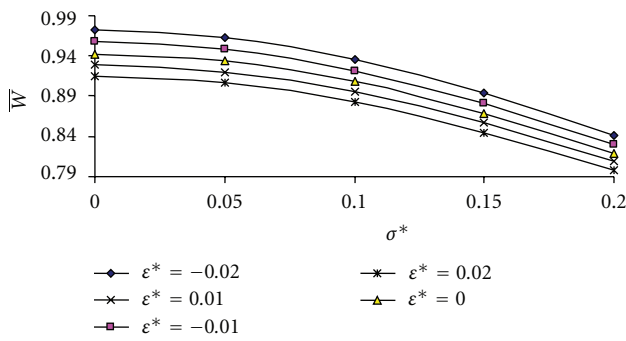
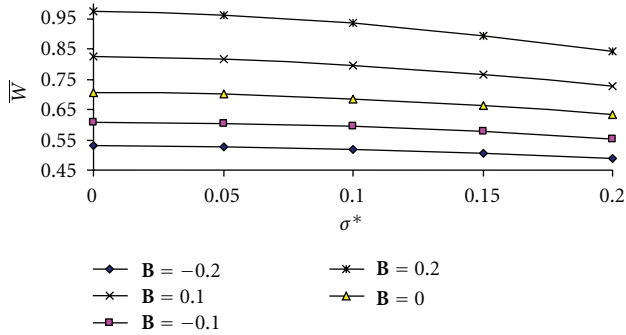
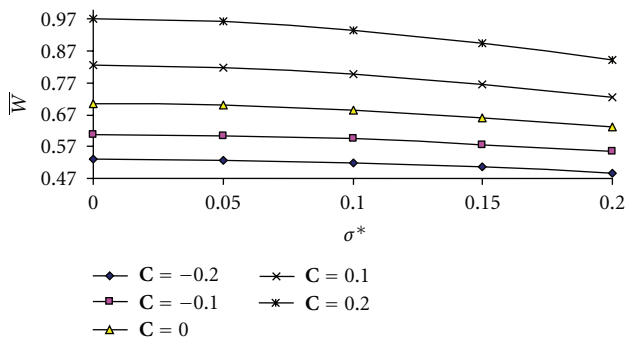
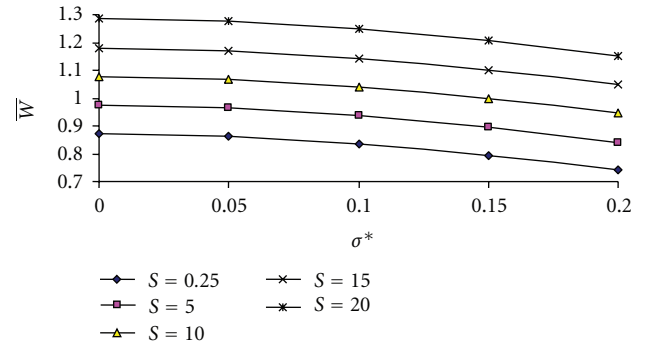
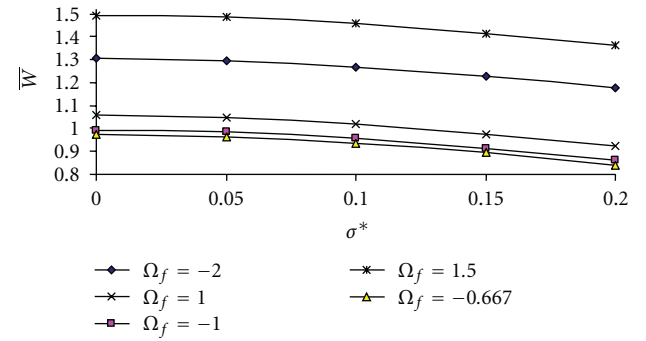
The bearing surfaces are assumed to be transversely rough. Following Christensen and Tonder [17–19] the thickness  $h(x)$  of the lubricant film is considered as

$$h(x) = \bar{h}(x) + h_s, \tag{1}$$

where  $\bar{h}(x)$  is the mean film thickness while  $h_s$  is the deviation from the mean film thickness characterizing the random roughness of the bearing surfaces. The deviation  $h_s$  is assumed to be stochastic in nature and described by the probability density function

$$f(h_s), \quad -c \leq h_s \leq c, \tag{2}$$

where  $c$  is the maximum deviation from the mean film thickness. The mean  $\alpha$ , the standard deviation  $\sigma$  and the

FIGURE 9: Load carrying capacity with respect to  $\sigma^*$  and  $\alpha^*$ .FIGURE 10: Load carrying capacity with respect to  $\sigma^*$  and  $\epsilon^*$ .FIGURE 11: Load carrying capacity with respect to  $\sigma^*$  and  $B$ .FIGURE 12: Load carrying capacity with respect to  $\sigma^*$  and  $C$ .FIGURE 13: Load carrying capacity with respect to  $\sigma^*$  and  $S$ .FIGURE 14: Load carrying capacity with respect to  $\sigma^*$  and  $\Omega_f$ .

parameter  $\epsilon$  which is the measure of symmetry associated with random variable  $h_s$  are defined by the relations

$$\begin{aligned}\alpha &= E(h_s), \\ \sigma^2 &= E[(h_s - \alpha)^2], \\ \epsilon &= E[(h_s - \alpha)^3],\end{aligned}\quad (3)$$

while  $E$  denotes the expected value given by the following:

$$E(R) = \int_{-c}^c Rf(h_s)dh_s, \quad (4)$$

where

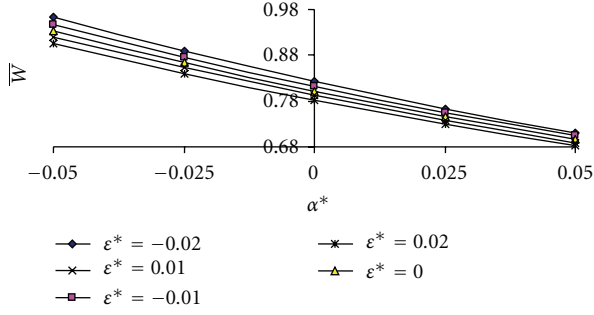
$$f(h_s) = \begin{cases} \frac{35}{32} \left(1 - \frac{h_s^2}{c^2}\right)^3, & -c \leq h_s \leq c \\ 0, & \text{otherwise.} \end{cases} \quad (5)$$

It is assumed that rotating upper plate lying along the surface determined by the following:

$$Z_u = h_0[\exp(-Br^2)]; \quad 0 \leq r \leq a, \quad (6)$$

approaching with normal velocity  $\dot{h}_0 = dh_0/dt$ , to the rotating lower plate lying along the surface

$$Z_l = h_0[\sec(-Cr^2) - 1]; \quad 0 \leq r \leq a, \quad (7)$$

FIGURE 15: Load carrying capacity with respect to  $\alpha^*$  and  $\varepsilon^*$ .

where  $h_0$  is central distance between the plates,  $B$  and  $C$  are the curvature parameters of the corresponding plates. The central film thickness  $h(r)$  then, is defined by the following:

$$h(r) = h_0[\exp(-Br^2) - \sec(-Cr^2) + 1]. \quad (8)$$

The lower and upper plate rotate with angular velocities is  $\Omega_l$  and  $\Omega_u$ , respectively.

Axially symmetric flow of the magnetic fluid between the plates is taken into consideration under an oblique magnetic field

$$\bar{H} = (H(r) \cos \phi(r, z), 0, H(r) \sin \phi(r, z)), \quad (9)$$

whose magnitude  $H$  vanishes at  $r = a$ ; for instance

$$H^2 = ka(a - r); \quad 0 \leq r \leq a, \quad (10)$$

where  $k$  is a suitably chosen constant so as to have a magnetic field of required strength, which suits the dimensions. The direction of the magnetic field plays a significant role since  $\bar{H}$  has to satisfy the relations (Agrawal [11], Bhat and Deheri [12])

$$\nabla \cdot \bar{H} = 0, \quad \nabla \times \bar{H} = 0. \quad (11)$$

Therefore,  $\bar{H}$  arises out of a potential function and the inclination angle  $\phi$  of the magnetic field  $\bar{H}$  with the lower plate is determined by the following:

$$\cot \phi \frac{\partial \phi}{\partial r} + \frac{\partial \phi}{\partial z} = \frac{1}{2(a - r)}, \quad (12)$$

whose solution is determined from the equation

$$c_1^2 \cos \varepsilon c^2 \phi = a - r, \quad z = -2c_1 \sqrt{(a - c_1^2 - r)}, \quad (13)$$

where  $c_1$  is a constant of integration.

The modified Reynolds equation governing the film pressure  $p$  then can be obtained as (Bhat and Deheri [12], (Patel et al. [29] and Prajapati [27])

$$\begin{aligned} & \frac{1}{r} \frac{d}{dr} \left\{ r g(h) \frac{d}{dr} \left( p - \frac{1}{2} \mu_0 \bar{\mu} H^2 \right) \right\} \\ & = 12 \mu \dot{h}_0 + \rho \left( \frac{3}{10} \Omega_r^2 + \Omega_r \Omega_l + \Omega_l^2 \right) \frac{1}{r} \frac{d}{dr} (r^2 g(h)), \end{aligned} \quad (14)$$

where

$$\begin{aligned} g(h) &= h^3 + 3h^2(\alpha^2 + \sigma^2) + 3h\sigma^2 + 3\sigma^2\alpha + \alpha^3 + \varepsilon, \\ \Omega_r &= \Omega_u - \Omega_l. \end{aligned} \quad (15)$$

Introducing the nondimensional quantities

$$\begin{aligned} \bar{h} &= \frac{h}{h_0}, \quad R = \frac{r}{a}, \quad \mu^* = -\frac{\mu_0 \bar{\mu} k h_0^3}{\mu h_0}, \\ P &= -\frac{h_0^3 p}{\mu a^2 h_0}, \quad \Omega_f = \frac{\Omega_l}{\Omega_u}, \\ \sigma^* &= \frac{\sigma}{h_0}, \quad \varepsilon^* = \frac{\varepsilon}{h_0^3}, \quad \alpha^* = \frac{\alpha}{h_0}, \\ \mathbf{B} &= B a^2, \quad \mathbf{C} = C a^2, \end{aligned} \quad (16)$$

and solving the associated Reynolds equation with the concerned boundary conditions

$$P(1) = 0, \quad \frac{dP}{dR} = -\frac{\mu^*}{2} \quad \text{at } R = 0, \quad (17)$$

one gets the expression for nondimensional pressure distribution

$$\begin{aligned} P &= \frac{1}{2} \mu^* R^2 (1 - R) \\ &\quad - 6 \int_1^R \frac{R}{G(h)} dR - \frac{S}{20} (3\Omega_f^2 + 4\Omega_f + 3) (1 - R^2), \end{aligned} \quad (18)$$

where

$$G(h) = \bar{h}^3 + 3\bar{h}^2 \alpha^* + 3\bar{h}(\alpha^* + \sigma^*) + 3\sigma^* 2\alpha^* + \varepsilon^* + \alpha^* 3. \quad (19)$$

The dimensionless load carrying capacity then, is given by the following:

$$\begin{aligned} \bar{W} &= -\frac{W h_0^3}{2\pi \mu a^4 h_0} \\ &= \frac{\mu^*}{40} + 3 \int_0^1 \frac{R^3}{G(h)} dR - \frac{S}{80} (3\Omega_f^2 + 4\Omega_f + 3), \end{aligned} \quad (20)$$

where the load carrying capacity  $W$  is obtained from the relation

$$W = 2\pi \int_0^a r p(r) dr. \quad (21)$$

### 3. Results and Discussions

It is clearly seen that the nondimensional pressure distribution and load carrying capacity are determined from (18), (20), respectively. It is also clear that these performance characteristics depend on various parameters such as  $\mu^*$ ,  $\sigma^*$ ,  $\alpha^*$ ,  $\varepsilon^*$ ,  $B$ ,  $C$ ,  $S$ , and  $\Omega_f$ . These parameters, respectively, show the effect of magnetic fluid lubricant, roughness,

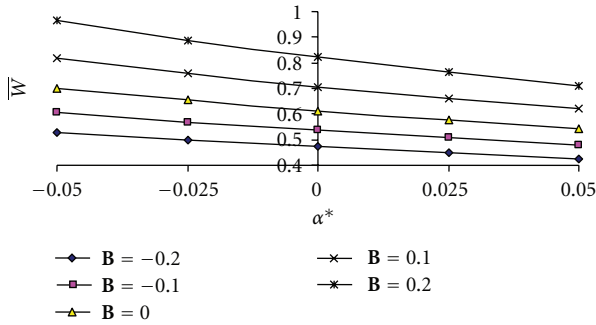


FIGURE 16: Load carrying capacity with respect to  $\alpha^*$  and B.

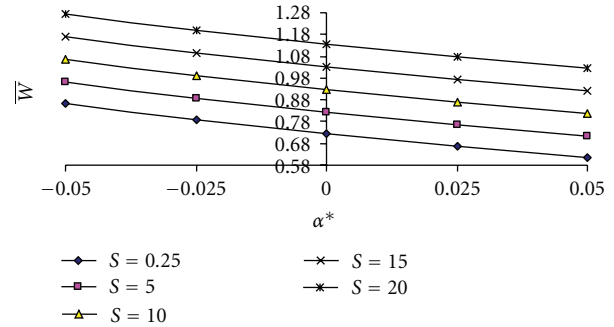


FIGURE 18: Load carrying capacity with respect to  $\alpha^*$  and S.

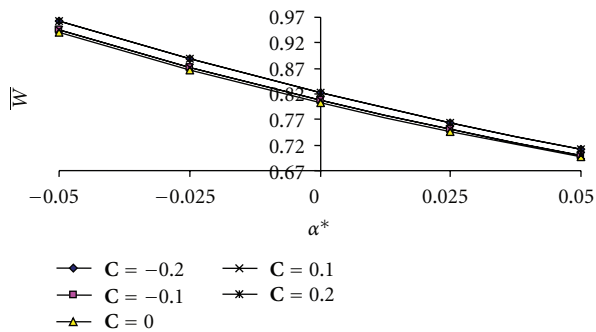


FIGURE 17: Load carrying capacity with respect to  $\alpha^*$  and C.

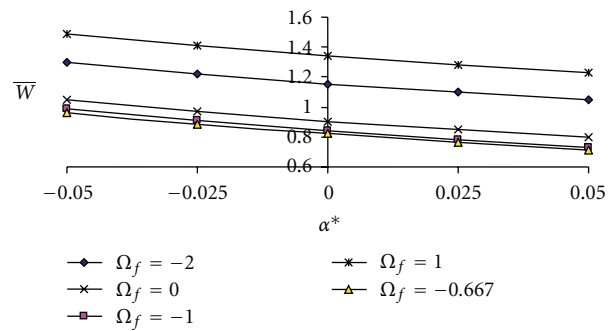


FIGURE 19: Load carrying capacity with respect to  $\alpha^*$  and  $\Omega_f$ .

curvature, and rotation, respectively. Taking the roughness parameters to be zero this study reduces to the corresponding magnetic fluid-based squeeze film performance in curved smooth rotating circular plates. Further, taking  $\mu^* = 0$  this discussion reduces to squeeze film performance in curved smooth rotating circular plates. Besides, in the absence of rotation this investigation gets reduced essentially to the performance of squeeze film between circular plates.

From (20) governing the distribution of load carrying capacity it is easily observed that the dimensionless load carrying capacity increases by  $\mu^*/40$  as compared to that of conventional lubricants. The variation of nondimensional load carrying capacity with respect to the magnetization parameter  $\mu^*$  is presented in Figures 2, 3, 4, 5, 6, 7, and 8 for various values of  $\sigma^*$ ,  $\alpha^*$ ,  $\varepsilon^*$ , B, C, S, and  $\Omega_f$ . These figures tend to indicate that the load carrying capacity increases significantly with respect to the magnetization parameter. It is noticed that among the roughness parameters the combined effect of the magnetization and skewness is more pronounced. However, the effect of  $\mu^*$  tends to be almost negligible at the initial stages (up to  $\mu^* = 0.05$ ). Furthermore, a symmetrical nature of the distribution of load carrying capacity is observed with respect to the lower plate's curvature parameter. The effect of  $\mu^*$  with respect to the lower plate's curvature parameter is almost negligible upto the value of  $\mu^* = 0.01$ .

Figures 9, 10, 11, 12, 13, and 14 depict the effect of standard deviation associated with the roughness on the distribution of load carrying capacity. It can be easily seen

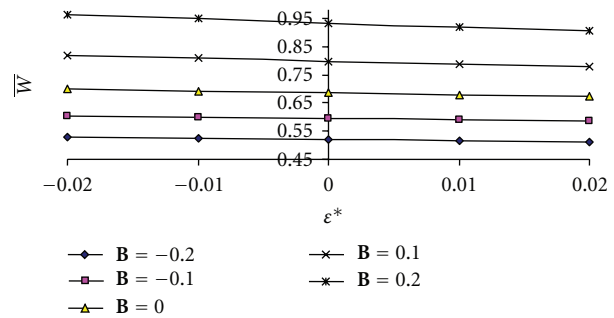


FIGURE 20: Load carrying capacity with respect to  $\varepsilon^*$  and B.

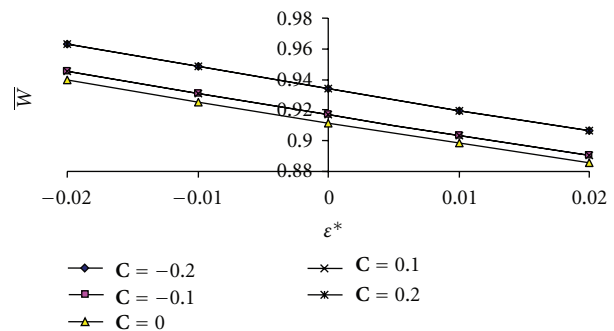


FIGURE 21: Load carrying capacity with respect to  $\varepsilon^*$  and C.

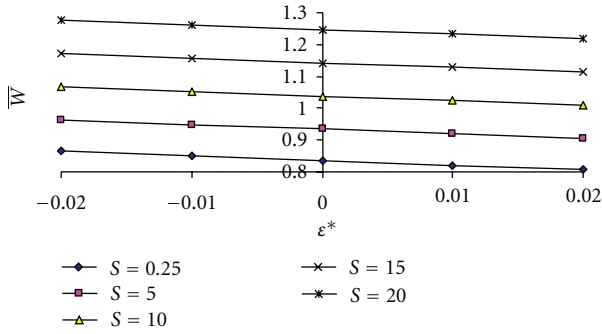


FIGURE 22: Load carrying capacity with respect to  $\epsilon^*$  and  $S$ .

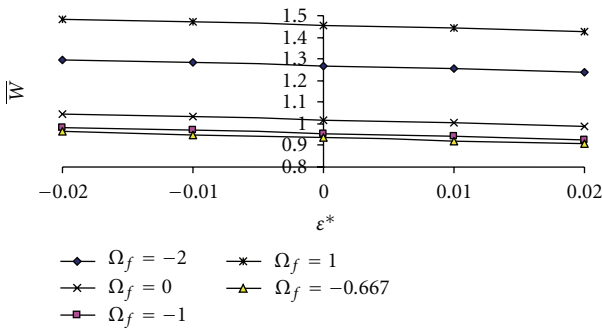


FIGURE 23: Load carrying capacity with respect to  $\epsilon^*$  and  $\Omega_f$ .

from these figures that the effect of standard deviation is basically adverse in the sense that the load carrying capacity decreases considerably. In addition, this negative effect of  $\sigma^*$  is relatively less in the case of upper plate's curvature parameter. Besides, the effect of rotational inertia with respect to the standard deviation is however negligible at the initial stage.

In Figures 15, 16, 17, 18, and 19 one can visualize the effect of variance on the distribution of load carrying capacity. These figures suggest that  $\alpha$  (+ve) decreases the load carrying capacity while  $\alpha$  (-ve) increases the load carrying capacity. Further, it is indicated that the combined effect of the upper plate's curvature parameter and the negative variance is significantly positive.

The effect of skewness on the distribution of load carrying capacity is given in Figures 20, 21, 22, and 23. As in the case of variance here also positively skewed roughness decreases the load carrying capacity while the load carrying capacity increases due to the negatively skewed roughness. Furthermore, there is manifest a symmetric distribution of the load carrying capacity with respect to the lower plate curvature parameter.

The combined effect of the curvature parameters is presented in Figure 24. It is easily seen that the upper plate's curvature parameter increases the load carrying capacity while effect of upper plate curvature parameter with respect to lower plate's curvature parameter is almost negligible.

Finally, the effect of rotation is presented in Figures 25, 26, 27, 28, and 29. It is clear that the effect of rotation is

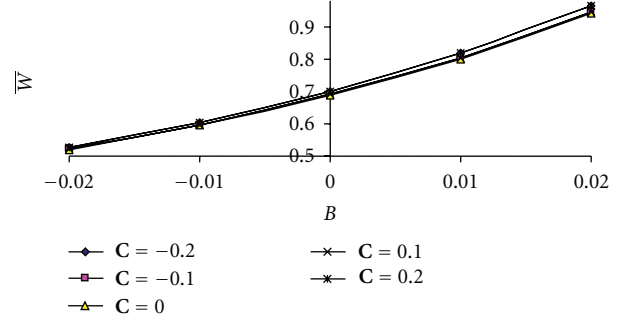


FIGURE 24: Load carrying capacity with respect to  $B$  and  $C$ .

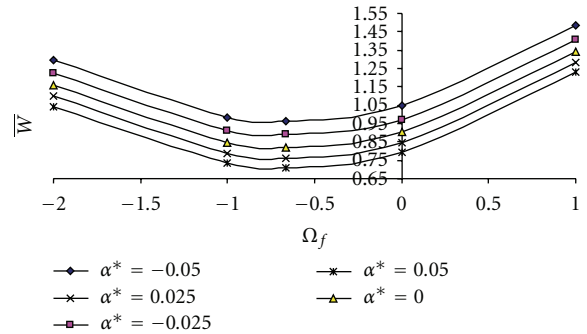


FIGURE 25: Load carrying capacity with respect to  $\Omega_f$  and  $\alpha^*$ .

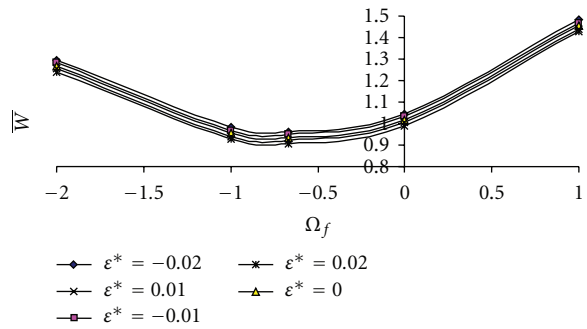


FIGURE 26: Load carrying capacity with respect to  $\Omega_f$  and  $\epsilon^*$ .

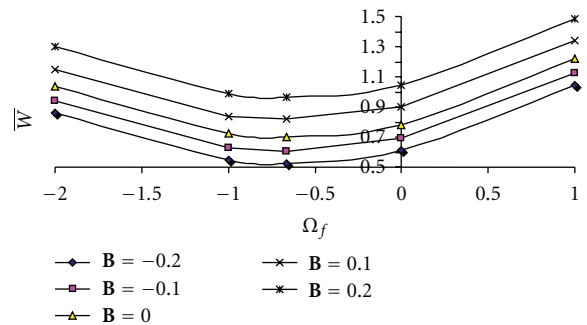


FIGURE 27: Load carrying capacity with respect to  $\Omega_f$  and  $B$ .

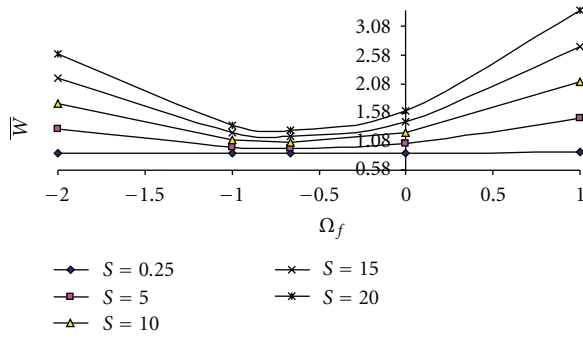


FIGURE 28: Load carrying capacity with respect to  $\Omega_f$  and  $S$ .

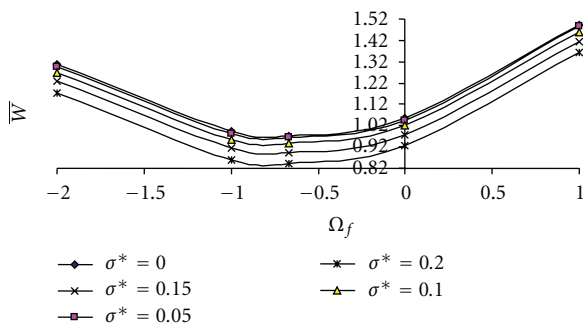


FIGURE 29: Load carrying capacity with respect to  $\Omega_f$  and  $\sigma^*$ .

quite sharp. One can observe that the effect of lower plate curvature parameter with respect to  $\Omega_f$  is almost negligible. It is established from these figures that the load carrying capacity decreases with respect to the rotation ratio  $\Omega_f$  upto the value  $\Omega_f = -0.667$  and afterwards the load carrying capacity increases. The rate of increase in load carrying capacity due to rotation is comparatively more in the case of lower plate curvature parameter while the rate of decrease with respect to  $\Omega_f$  is more in the case of rotational inertia  $S$ .

Some of these figures indicate that the increased load carrying capacity due to upper plate's curvature parameter gets further increased in the case of negatively skewed roughness and this further enhances when negative variance occurs. It is revealed that the negative effect induced by the transverse surface roughness can be compensated upto some extent by the magnetization parameter choosing a suitable combination of curvature parameter and rotation ratio parameter in the case of negatively skewed roughness.

A comparison of the results presented here and the discussion of Patel and Deheri [15] indicates that at least the load carrying capacity increases by 3% to 4% in spite of the fact that the roughness has an adverse effect on the performance of bearing system. Further, in view of the deliberations of Patel and Deheri [14] of our article are provided and additional degrees of freedom in terms of the ratio of the curvature parameter for improving the performance of the squeeze film.

## 4. Conclusion

This investigation makes it clear that the roughness merits a serious attention while designing this magnetic fluid based bearing system even if suitable values of curvature parameter and rotation ratio are chosen. This is all the more important from the bearings life period point of view. In addition, the bearing can support a load even in the absence of flow unlike the case of a conventional lubricant.

## Nomenclature

- $a$  : Radius of the upper plate
- $b$  : Radius of the lower plate
- $k$  : Aspect ratio
- $p$  : Pressure
- $B$  : Curvature parameter of the upper plate
- $C$  : Curvature parameter of the lower plate
- $H$  : Magnitude of the magnetic field
- $P$  : Nondimensional pressure
- $W$  : Load carrying capacity
- $c_1$  : Constant of integration
- $h_0$  : Central distance
- $\dot{h}_0$  : Normal velocity
- $\bar{W}$  : Nondimensional load carrying capacity
- $\mu$  : Fluid viscosity
- $\sigma$  : Standard deviation
- $\varepsilon$  : Skewness
- $\alpha$  : Variance
- $\phi$  : Inclination angle
- $\mu_0$  : Free space permeability
- $\bar{\mu}$  : Magnetic susceptibility
- $\mu^*$  : Magnetization parameter.

## Acknowledgment

The constructive suggestions, critical remarks, and in-depth comments of referees leading to overall improvement on the presentation of the paper are gratefully acknowledged.

## References

- [1] F. R. Archibald, "Load capacity and time relations for squeeze films," *ASME*, vol. 78, pp. A231–A245, 1956.
- [2] D. F. Hays, "Squeeze films for rectangular plates," *ASME*, vol. 58, pp. 243–248, 1963.
- [3] Murti .PR.K., "Squeeze films in curved circular plates," *ASME Transactions, Journal of Lubrication Technology*, vol. 97, no. 4, pp. 650–652, 1975.
- [4] M. B. Ajwalya, *On certain theoretical studies in hydrodynamic and electro magnetohydrodynamic lubrication [Ph.D. thesis]*, S. P. University, V. V. Nagar, 1984.
- [5] R. M. Patel and G. M. Deheri, "Analysis of the behaviour of the squeeze film between curved plates," *The Journal of the Indian Academy of Mathematics*, vol. 24, no. 2, pp. 333–338, 2002.
- [6] J. Prakash and S. K. Vij, "Load capacity and time-height relations for squeeze films between porous plates," *Wear*, vol. 24, no. 3, pp. 309–322, 1973.
- [7] H. Wu, "The squeeze film between rotating porous annular disks," *Wear*, vol. 18, no. 6, pp. 461–470, 1971.

- [8] M. V. Bhat and K. C. Patel, "The effect of axial-current-induced pinch on the lubrication of rotating porous annular and circular discs," *Wear*, vol. 50, no. 1, pp. 39–46, 1978.
- [9] K. H. Vora and M. V. Bhat, "The load capacity of a squeeze film between curved porous rotating circular plates," *Wear*, vol. 65, no. 1, pp. 39–46, 1980.
- [10] P. D. S. Verma, "Magnetic fluid-based squeeze film," *International Journal of Engineering Science*, vol. 24, no. 3, pp. 395–401, 1986.
- [11] V. K. Agrawal, "Magnetic-fluid-based porous inclined slider bearing," *Wear*, vol. 107, no. 2, pp. 133–139, 1986.
- [12] M. V. Bhat and G. M. Deheri, "Squeeze film behaviour in porous annular discs lubricated with magnetic fluid," *Wear*, vol. 151, no. 1, pp. 123–128, 1991.
- [13] M. V. Bhat and G. M. Deheri, "Magnetic fluid based squeeze film between two curved circular plates," *Bulletin of Calcutta Mathematical Society*, vol. 85, pp. 521–524, 1993.
- [14] R. M. Patel and G. M. Deheri, "behaviour of the squeeze film between annular plates," *The Journal of Engineering and Technology*, vol. 16, pp. 50–53, 2003.
- [15] R. M. Patel and G. M. Deheri, "Magnetic fluid based squeeze film between two curved plates lying along the surfaces determined by secant functions," *Indian Journal of Engineering and Materials Sciences*, vol. 9, no. 1, pp. 43–48, 2002.
- [16] S. T. Tzeng and E. Saibel, "Surface roughness effect on slider bearing lubrication, Transaction," *ASME Transactions, Journal of Lubrication Technology*, vol. 10, pp. 334–338, 1967.
- [17] H. Christensen and K. C. Tonder, "Tribology of rough surfaces: stochastic models of hydrodynamic lubrication," SINTEF Report 10/69-18, 1969.
- [18] H. Christensen and K. C. Tonder, "The hydrodynamic lubrication of rough bearing surfaces of finite width," in *ASME-ASLE Lubrication Conference*, Cincinnati, Ohio, USA, 1970, paper no. 70-Lub-7.
- [19] H. Christensen and K. C. Tonder, "Tribology of rough surfaces: parametric study and comparison of lubrication models," SINTEF Report 22/69-18, 1969.
- [20] K. C. Tonder, "Surface distributed waviness and roughness," in *First World Conference in Industrial Tribology*, vol. 3, pp. 1–8, 1972.
- [21] L. L. Ting, "Engagement behaviour of lubricated porous annular disks. Part1: squeeze film phase, surface roughness and elastic deformation effects," *Wear*, vol. 34, pp. 159–182, 1975.
- [22] J. Prakash and K. Tiwari, "Roughness effects in porous circular squeeze-plates with arbitrary wall thickness," *Journal of Lubrication Technology*, vol. 105, no. 1, pp. 90–95, 1983.
- [23] B. L. Prajapati, "Behavior of squeeze film between rotating porous circular plates: surface roughness and elastic deformation effects," *Pure and Applied Matematika Sciences*, vol. 33, no. 1-2, pp. 27–33, 1991.
- [24] S. K. Guha, "Analysis of dynamic characteristics of hydrodynamic journal bearings with isotropic roughness effects," *Wear*, vol. 167, no. 2, pp. 173–179, 1993.
- [25] J. L. Gupta and G. M. Deheri, "Effect of roughness on the behavior of squeeze film in a spherical bearing," *Tribology Transactions*, vol. 39, no. 1, pp. 99–102, 1996.
- [26] P. I. Andharia, J. L. Gupta, and G. M. Deheri, "Effect of transverse surface roughness on the behavior of squeeze film in a spherical bearing," *Journal of Applied Mechanics and Engineering*, vol. 4, pp. 19–24, 1999.
- [27] B. L. Prajapati, "Squeeze film behaviour between rotating porous circular plates with a concentric circular pocket: surface roughness and elastic deformation effects," *Wear*, vol. 152, no. 2, pp. 301–307, 1992.
- [28] J. R. Lin and C. F. Chinang, "Effects of surface roughness and rotational inertia on the optimal stiffness of hydrostatic thrust bearings," *International Journal of Applied Mechanics and Engineering*, vol. 7, no. 4, pp. 1247–1261, 2002.
- [29] H. C. Patel, G. M. Deheri, and R. M. Patel, "Performance of Magnetic fluid based rotating rough circular step bearing," *International Journal of Applied Mechanics and Engineering*, vol. 13, no. 2, pp. 441–455, 2008.



**Hindawi**

Submit your manuscripts at  
<http://www.hindawi.com>

